Computer Aided Surgery 7:342–352 (2002)

Biomedical Paper

Three-Dimensional Image Registration of Phantom Vertebrae for Image-Guided Surgery: A Preliminary Study

Diane M. Muratore, Ph.D., Jeannette Herring Russ, Ph.D., Benoît M. Dawant, Ph.D., and Robert L. Galloway, Jr., Ph.D.

Departments of Biomedical Engineering (R.L.G.), Electrical Engineering and Computer Science (J.H.R., B.M.D.), and Neurological Surgery (R.L.G.), Vanderbilt University, Nashville, Tennessee, and Department of Biomedical Engineering (D.M.M.) Western New England College, Springfield, Massachusetts

ABSTRACT

Objective: Applications of three-dimensional ultrasound (3D US) are emerging throughout the field of medicine. In this study, tracked, free-hand 3D phantom US images were mapped to computed tomograms (CT) as a development for image-guided surgery (IGS) of the spine. In the operating room, the registration of tracked 3D US images to other imaging modalities, such as CT, could allow the surgeon to identify more precisely the surgical target area prior to the incision. An independent quantitative measure of registration accuracy using a fiducial marker system was provided.

Methods: Three-dimensional free-hand US images of a phantom spine were created by tracking the transducer with an optical sensing system. Two sets of images were acquired from three lumbar vertebrae using 4.5- and 7.5-MHz transducers. These images were then segmented for the extraction of the posterior vertebral surface. Next, a surface-based registration of US to the corresponding segmented CT images was performed. Registration errors were computed as the distance between a set of target points transformed using the experimental transformation and the same set of target points transformed using fiducial markers as a gold standard.

Results: Results indicated that alignment of these image sets is feasible using only part of the vertebral surface. In particular, the regions of the spinous process and laminae were used for registration. Target registration errors (TREs) were found to be lowest using the highest resolution CT images. Using the CT scans with 2-mm slice thickness, the TRE was calculated to be 1.33 ± 0.30 mm for the 7.5-MHz US data set and 2.81 ± 0.10 mm for the 4.5-MHz US data set. Moreover, residual errors in these surface alignments were 0.69 ± 0.18 mm and 0.61 ± 0.20 mm for the 4.5- and 7.5-MHz sets, respectively.

Conclusion: A rigid, surface-based registration of CT images to phantom spinal US images, acquired with a free-hand, tracked transducer, is achievable with a limited, easily obtainable portion of the vertebral surface. Comp Aid Surg 7:342–352 (2002).

Key words: **image-guided surgery; spine; 3D ultrasound; CT; image registration**

INTRODUCTION

The aim of this work is to quantitatively register phantom spinal ultrasound (US) images to corresponding CT images, with the ultimate goal of providing guidance in closed-back spinal therapies.

Received September 19, 2000; accepted November 27, 2002.

Address correspondence/reprint requests to: Diane Muratore, Western New England College, School of Engineering, 1215 Wilbraham Road, Springfield, MA 01119. E-mail: dmurator@wnec.edu

This article is an expansion of research presented at the SPIE Medical Imaging conference in San Diego, CA, February 2000.

Published online in Wiley InterScience (www.interscience.wiley.com). DOI: 10.1002/igs.10055

When medical images and tracked surgical instrumentation are registered to a universal, physical-space coordinate frame, explicit positional information for locating surgical targets can be determined. Our proposed method of surgical guidance consists of registering percutaneous spinal US images, acquired with a free-hand, optically tracked US transducer, to preoperative CT scans. As a means of registering these preoperative spinal images to the physical space of the patient and operating room, we have tested in a phantom model the use of registered 3D vertebral US images to obtain the necessary spatial transformations. Each 3D US volume was created by compounding a series of tracked, free-hand 2D US scans. Registration accuracy was objectively measured using a gold-standard fiducial marker technique.

Ultrasound has been recommended by medical experts as the imaging modality having the greatest potential for aiding in image-to-physical-space registration for spinal procedures. This statement was made in the 1999 *Report of the Image-Guided Spine Procedures Workshop.* Here, several teams of researchers and physicians reported their recommendations for the various technical aspects of a spinal surgery. In particular, the researchers believed that a 3D geometrical model of the spine surface, constructed from a cloud of US points, could lead to more accurate registrations.[1]

The image registration procedure required in IGS can be undertaken using a variety of techniques, including point-based, surface-based, or intensity-based registrations. The literature suggests that surface-based techniques perform best in cases of image registration for the spine. In a 1998 review of image registration techniques, Maintz and Viergever reported that almost all nonclinical cases of spinal image registration have involved surface-based methods.[2] Among the published clinical cases involving spinal image registration, surface-based approaches continue to perform better than other methods.

In previous research conducted by our laboratory,[3] a surface-based registration of physical vertebral surface points to segmented phantom spinal CT images was performed using the Besl-McKay iterative closest point (ICP) algorithm. An accurate registration was achievable using only certain patches of the vertebral surface. In particular, the spinous process and laminae produced the best registration results among various combinations of vertebral surface patches. Conveniently, these two surface regions fall within the field of view of a vertebral US image acquired axially. To maintain consistency with this previous work, we again used the ICP method to align the US images to CT images in the present study.

Previous reports have found some success for IGS in spinal surgeries. For instance, spinal image registration has been tested clinically by researchers at the University of Toronto. Using cadaveric lumbar spines, they found that a surface-matching approach produced better overall accuracy than a strictly point-based method when registering physical points of the vertebral surface to CT spinal images. A 1.2-mm error was reported as the average distance between planned and resulting entry points for pedicle screw insertions.[4]

The use of IGS has been particularly effective in increasing the accuracy of spinal fixation hardware, where erroneous insertion of pedicle screws is known to occur in up to 31% of cases.[5] Fortunately, the introduction of technological guidance in these procedures has been shown to improve pedicle screw placements in 87–95% of cases.[6–8] A report of one of the first human-model trials of IGS in the spine using image registration was published in late 1999.[9] In that study, a group from Bristol, England, applied registered pre- and intraoperative CT images to resect portions of the anterior cervical spine and to insert cervical screws. They reported a successful registration for 70% of their procedures with a mean registration accuracy of 0.74 ± 0.40 mm. This accuracy was determined by their image-guidance system, the StealthStation® (Sofamor Danek, Memphis, TN), and was not an independent measure of accuracy.[9]

On the whole, however, the application of tracked, free-hand 3D US for spinal surgeries has been studied by only a few research groups.[3,10] One team from Grenoble, France, has actively researched the application of tracked 3D US to image-guided spinal procedures over the past decade, and in 1996 reported their work in anatomy-based registration from phantom studies of an isolated vertebra.[10] They reported that intraoperative surface data could be collected from a vertebral phantom using a 2D US probe that was optically localized in three dimensions. In these studies, the region of interest was an isolated, single vertebra, and the reference emitter was affixed to the spinous process of this vertebra. This setup compensated for any effects due to vertebral motion. The group reported that their registration algorithm achieved a residual error on the order of 1 mm.[10] More recently, this group has demonstrated the use of US registration to place iliosacral screws in the pelvic ring. Using a 3D CT model of the pelvis, optimal

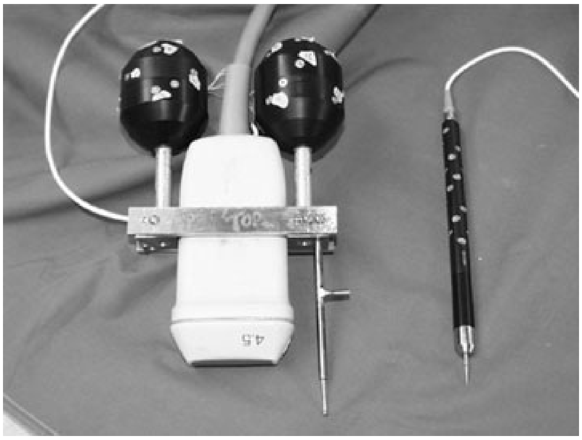

Fig. 1. The tracked 4.5-MHz transducer (left) and the tracked pointer (right).

drilling trajectories were planned, then the screws were placed. This method was compared to a standard surface-based registration for accuracy of screw placement, although only a qualitative measure was provided, noting success in 12 of 12 cases.[11]

Tracked, free-hand 3D US has also been studied in a phantom model at the University of Washington for use in image-guided neurosurgery. A point-based algorithm was used to register US and MR images from a custom-made phantom. Registration results were dependent on the distance of their target from the US transducer. With a target placed at a depth of 6 cm in a 3.5-MHz sector scan, this point was registered to a corresponding point in MR space with an accuracy of 2.00 ± 0.75 mm.[12]

METHODS

Image Acquisition

Ultrasound images were scanned from the lumbar portion of a life-size plastic phantom spine that was immersed in a water tank. Two image sets were collected from the L1 to L3 vertebrae along the longitudinal axis of the spine using two different free-hand, tracked transducers of center frequencies 4.5 and 7.5 MHz. An optical tracking device was mounted to the back end of the transducer that functions in conjunction with the Optotrak® system (Northern Digital, Ontario, Canada). The B-mode instrumentation from a Hewlett-Packard SONOS 1000® US machine was used to acquire 30 images at each vertebral level. Figure 1 shows the tracked US transducer and a tracked pointer (used in accuracy measurements).

The US beam of the tracked transducer was calibrated in 3D space using only the two devices in Figure 1. With the transducer's tracking system serving as a reference emitter, the tracked pointer was moved in and out of the US beam at multiple locations throughout the beam. Throughout this process, images and positional information of the pointer were stored simultaneously. According to this procedure, all of the pixels in the US beam were defined in 3D space to within 0.4 mm. Additional information about the calibration procedure can be found in ref. 13.

CT images were collected from the same plastic phantom spine using a Siemens Somatom Plus® scanner. These images were obtained in the transverse plane at three different slice thicknesses: 2, 3, and 5 mm. A set of five imaging markers was positioned on each vertebral body during the scanning; these markers serve as gold-standard fiducial points, and are used in the accuracy estimations. Each CT image set contains slices of 512×512 voxels, with the voxel dimensions in millimeters being $0.245 \times 0.245 \times$ slice thickness.

Imaging Markers

Prior to the collection of any image data, five small plastic posts were drilled into each lumbar vertebra of the phantom spine. These posts are 7 mm in length and 5 mm in diameter. Cylindrical imaging markers were clipped on the posts prior to acquisition in CT, then removed when US images were acquired. The centroid of the cylindrical marker defines the position of the marker in space. An established method for accurate localization of imaging markers in CT was applied to identify the centroids in our CT image sets.[14] By replacing the imaging marker with a hemispherical divot cap, the location of the marker in physical space can be identified to within 0.3 mm using a tracked pointer. When the tip of a tracked pointer is inserted into the divot, the center of the tip corresponds to the centroid of the marker. This feature allows for accurate point-based registrations by matching corresponding centroids. A target registration error of approximately 0.7 mm is achievable using this point-based marker method.

These imaging markers were used solely for accuracy assessment in this study. This point-based accuracy measurement is offered as a means of predicting the outcome of future clinical trials that would be conducted without the use of external markers. The markers are manufactured by Z-Kat, and have been shown to be very effective in registering various imaging modalities under numerous registration methods.[15] Figure 2 shows the imaging

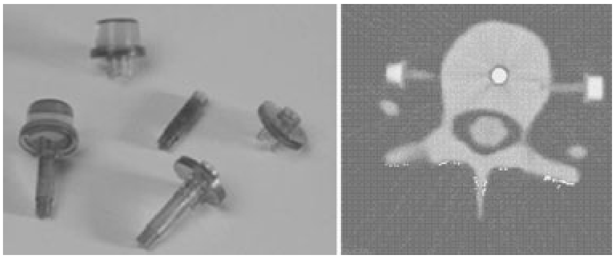

Fig. 2. Left: acustar imaging markers. Right: imaging markers as they appear in a CT slice.

markers and a slice of CT data with the markers inserted.

Before the US images were acquired, the divot caps were placed on the posts and their physical space location was recorded. The positions of the divot caps were collected in the same physical-space reference frame (RB_0) as the tracked US images. This information permitted us to perform a point-based registration from the physical space of the reference coordinate system to CT image space. Because only the divot caps and not the imaging markers were collected in RB_0 space, this point-based registration is a true estimate of accuracy. A more detailed description of our error assessment is given in a later section.

Image Segmentation

The implementation of a surface-based registration between multimodal image sets requires the segmentation of surface regions from the scans of interest. The steps involved in segmenting the US images include the applications of (1) a morphological open operator, (2) a linear threshold of intensity, (3) a ray-tracing algorithm, and finally (4) a conversion of these surface points to 3D points in the reference coordinate frame RB_0. The vertebral regions of interest that remain after the segmentation are the laminae and the spinous process, given as a cloud of surface points. Sample 4.5-MHz US images prior to and after processing are shown in Figure 3.

The list of extracted US points was subdivided into two sets: a fiducial set and a target set. The fiducial point cloud (set F) is used to find the experimental surface-based transformation, and the target set (set T) is used in the accuracy estimation. Basically, the target set is a subset of the entire US surface point set; it consists of arbitrarily selected surface points that are held out of the surface-based registration process. Once the registration process is complete, the test set is used in computing the TRE.

A modification of the Marching Cubes algorithm[16–18] was applied to the sets of CT tomographs to represent the vertebral surface. This algorithm creates a manifold surface defined by a set of triangles. Triangle vertices are located along the edges of five tetrahedra that are associated with a cube formed from eight neighboring voxels. The algorithm proceeds by analyzing each cube (or "8-cell") in the image and placing triangle vertices wherever a user-defined intensity level crosses the edge of a tetrahedron. The algorithm requires only one intensity parameter for proper execution. Because the Hounsfield number of the phantom's plastic composite is approximately an order of magnitude greater than that of the other image features, the conditions are favorable for creating a near-ideal iso-surface with this algorithm.

Rigid Registration

We used a rigid, surface-based registration method[19,20] for aligning the sets of vertebral surfaces, because the regions of interest (ROIs) are rigid, bony surfaces. As the spine is only piecewise rigid at the level of each vertebra, the image reg-

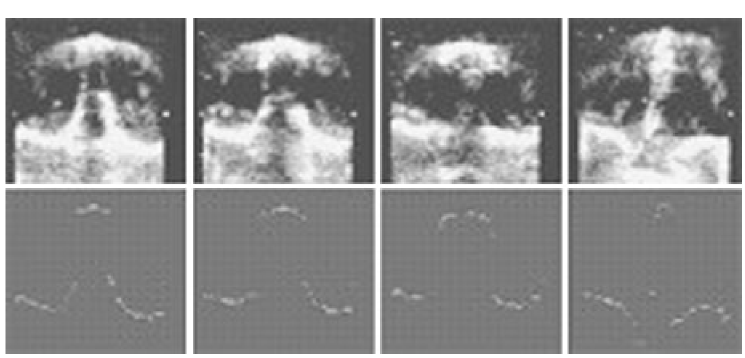

Fig. 3. Series of US images with their corresponding extracted surfaces.

istration for this application is performed on a vertebra-by-vertebra basis. Because of the distinct vertebral shape, there is no rotational symmetry in any plane of a vertebral scan. Therefore, the pitfalls of a surface-based registration method that are encountered when registering brain images can be minimized in the case of registration of a complete vertebral scan.

The surface-matching algorithm that we applied was an independent implementation of the Besl-McKay ICP algorithm.[19,20] One option for using the ICP algorithm seeks a best-fit solution in aligning corresponding points and surfaces in two different sets. In our specific case, the extracted points from one surface (US) were aligned with the triangle-set representation of the other surface (CT). The ICP algorithm functions with two steps. First, for each point in the US set F, a closest point in the CT set is found. Next, a transformation is computed that maps these two point sets. This surface-matching process iterates until a stopping criterion is met. The algorithm converges to a local minimum of a cost function, which is the root mean square (RMS) distance of corresponding points at the last iteration. The output from the ICP algorithm is a 4×4 transformation matrix that integrates the six optimized parameters: three rotation parameters about the x-, y-, and z-axes, and three translation parameters in the x-, y-, and z-directions. In our case, we called the transformation T_{BM}. The ICP approach performs best when the inputs to the algorithm are initially rotated and translated to a position that is near to the expected solution.

To address this issue of initial alignment, we used a point-based approach to derive the initial transformation. Four representative points were selected from the vertebral surface, essentially intrinsic fiducial markers, although their positions were not chosen from predetermined locations. Points on both the CT surface and the US surface were chosen from the following regions for each vertebra: the top of the spinous process, the front right lamina, the rear right lamina, and the center left lamina. The geometry of these four selected points ensures that any problems due to symmetry will be avoided. Furthermore, this point-based procedure for initially aligning the image sets is a process that can be mimicked in surgical cases.

A singular-value decomposition (SVD) algorithm was applied to find the best match of the four points. The transformation that was produced here, T_{init}, was employed in the transformation of the entire US point set F into CT image space. Next, these transformed US points and the vertices of the CT triangulated surface were put into the ICP algorithm and allowed to converge to a solution. The output transformation, T_{BM}, is the final solution to the surface-based registration.

Error Computation

A hold-out technique was used to quantify the registration error in this study. The target points in US set T were held out from the points used to find the surface-based transformation, so they were consequently used only in error estimation. The target points in set T were mapped into CT space using the two different transformations from (1) the surface-based registration, and (2) the gold-standard registration.

Using the gold-standard approach, the centroids of the divot caps in physical space were matched to those of the imaging markers in CT space. This point-based registration, T_{gold}, served as a gold standard by which we would compare the results of the surface-based registration. We used an SVD solution to find the point-based transformation between the 3D physical space of US (RB_0) and CT image space. On the other hand, in the surface-based image registration, we aligned the US point cloud of set F with the corresponding CT surface set. From this registration, the transformation matrix T_{BM} was produced.

In a perfect scenario, the two sets of transformed target points would be in precisely the same locations after undergoing these transformations. In a more realistic scenario, the error in misalignment of the data under the two transformations can be calculated as the average RMS distance between corresponding points in the two transformed target sets. This error is termed the target registration error or TRE. Figure 4 depicts the steps with which the error is calculated in our registration process.

RESULTS

In aligning the US points to the CT vertebral surfaces, we were able to achieve good qualitative and quantitative results, especially with the CT data set having a 2-mm slice thickness. We observed that registration quality improved as CT resolution increased. Figure 5 demonstrates the type of consistent qualitative results that were observed from this surface-based registration. The US points in this figure were extracted from images obtained with the 7.5-MHz transducer. Figure 5a shows the US points of set F prior to registration projected onto the corresponding CT slice from L2. The US points appear as small white dots on the top of the verte-

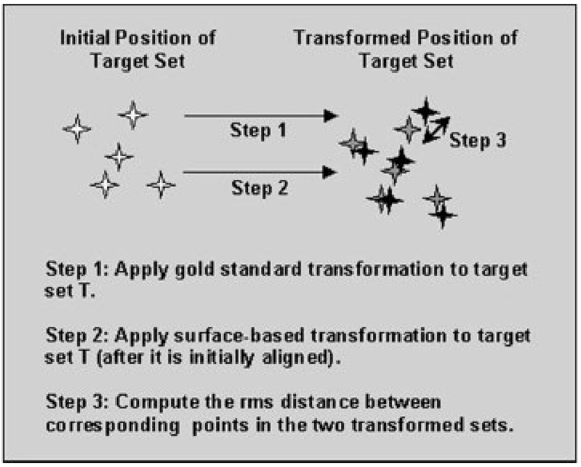

Fig. 4. Diagram depicting the method for target registration error calculation.

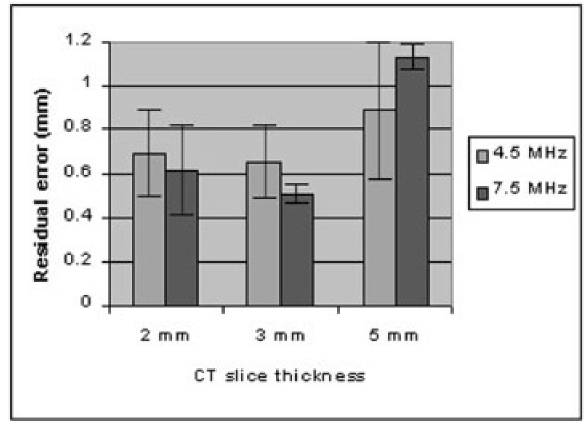

Fig. 6. Average residual error in registering US to CT for three lumbar vertebrae.

bra in the areas of the spinous process and laminae. The relatively close surface match is exemplified in Figure 5b, where the registered US points smoothly follow the vertebral contour in the CT slice.

Quantitatively, in registering US to the 2-mm and 3-mm CT scans, the residual errors of roughly 0.5–0.7 mm showed that the US fiducial points in set F found closely matching points on the CT surface. Residual error is a measure of the average distance between the surfaces in the two registered sets. The graphs in Figure 6 indicate that the vertebral US point cloud almost always fell within 1 mm of the CT surface. In this series of bar graphs, the residual errors were averaged for the surface matching of the three lumbar vertebrae scanned at both transducer frequencies, and the three plotted groups represent the residual error values for the registrations at the three different CT slice thicknesses. Approximately 83% of the 18 individual registration trials yielded residual errors under 1 mm, and two-thirds of these trials resulted in residual errors under 0.6 mm. Residual error was highest in registering the US points to the 5-mm CT data set. Nevertheless, the maximum residual error was 1.57 mm in aligning the 4.5-MHz set on the L1 vertebra of the 5-mm CT scans; the minimum residual error was 0.46 mm, which came from fitting the 7.5-MHz points to the 2-mm CT set on L1.

Using the transformations derived from the surface-based registration and the gold-standard registration (T_{BM} and T_{gold}, respectively), the US target points were matched to the targets in CT. In Figure 7, the target registration errors were averaged for all three vertebral levels for both transducer frequencies at the three different CT slice thicknesses. The TRE values from the 7.5-MHz data set were significantly better than those of the 4.5-MHz set in the case of the alignment to the 2-mm and 3-mm CT sets. Nonetheless, all of the

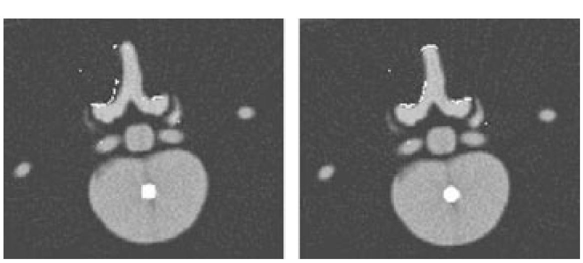

Fig. 5. Left: Preregistered US points on a 2-mm slice of CT data from L2. Right: Registered US points on the same slice of CT data from L2.

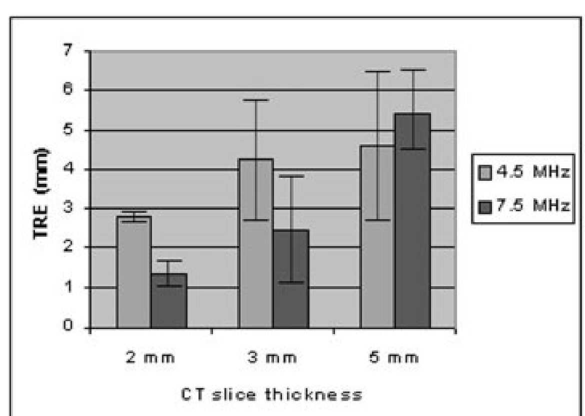

Fig. 7. Average target registration error in registering US to CT for three lumbar vertebrae.

Table 1. Rotations and Translations Yielded by the Surface-Based Registration of the US Fiducial Points to the 2-mm CT set

Frequency	Vertebra No.	R_x (°)	R_y (°)	R_z (°)	Distance between centers (mm)
4.5 MHz	L1	1.3	7.8	5.3	0.54
4.5 MHz	L2	−10.4	−23.8	5.1	0
4.5 MHz	L3	−5.2	−11.1	0.6	−3.21
7.5 MHz	L1	−2.6	−28.0	8.1	−1.54
7.5 MHz	L2	11.0	−28.7	12.6	−1.45
7.5 MHz	L3	−1.5	18.2	0.6	−2.45

Values are given as the difference prior to and after registration.

registration trials with the 2-mm CT scans produced TREs under 3 mm. In general, the average TRE from both transducer sets increased as CT resolution decreased. The best overall TRE was produced in registering the 7.5-MHz US target points to the 2-mm CT set; this target set matched its corresponding points with an average TRE of 1.33 ± 0.30 mm. Similarly, the 2-mm CT set yielded the best TRE for the 4.5-MHz points with a value of 2.81 ± 0.10 mm. The maximum TREs occurred when registering to the CT scans with the lowest resolution. Here, average TREs were measured at 4.60 ± 1.85 mm and 5.43 ± 0.94 mm for the 4.5- and 7.5-MHz sets, respectively. Overall, the smallest, individual-case TRE resulted from aligning the 7.5-MHz point cloud of L1 to the 2-mm CT scans, producing a TRE of 0.98 ± 0.09 mm. The minimum TRE for the 4.5-MHz registrations came from aligning the US points of L2 to the 3-mm CT tomograms, resulting in a TRE of 2.57 ± 0.11 mm.

The individual TRE values for the 7.5-MHz data set ranged from 0.98 to 1.52 mm for surface matching of the three different vertebrae in the 2-mm CT set. On the other hand, the TRE values for registering the 4.5-MHz data to the same CT set had a smaller range yet greater magnitude, ranging from 2.67 to 2.91 mm. The variability in TRE tended to increase as the CT resolution decreased.

DISCUSSION AND CONCLUSION

Most surface-based registration approaches call for some initial alignment scheme to put the two surfaces in generally the same space. One method for tackling the initial alignment problem could involve the mapping of principal axes. The principal axes approach is, however, difficult to manage with partial data sets, such as the US surface points from this study. Therefore, although the point-based approach applied in this study requires user input, the method is a practical and efficient solution to the initial alignment issue.

As a demonstration that the computed initial alignment was suitable for registration of our data, the magnitude of the rotation and translation parameters in the output transformation matrices were examined. This computation showed that the registration algorithm was not very sensitive to initial position, having rotated the cloud of fiducial US points by as much as 28.7° about one axis and having translated the fiducial points by as much as 3.2 mm from their starting position. The results in Table 1 were produced from the surface-based registration with the 2-mm CT surface set. The rotations about the x-, y-, and z-axes are listed in degrees as R_x, R_y, and R_z, respectively. The translation of the centers of the four points used in initial alignment was found for each vertebra prior to and after the surface-based registration. The Cartesian difference between these locations is presented in Table 1 as the distance between the centers. The small translation values suggest that four quickly selected anatomic locations can center the translation accurately. The large angles suggest that the subsequent surface registration is robust in the face of relatively large angular corrections. Given the better resolution in this CT data set compared to that in the other CT sets used in this study, the transformations produced by these registrations yielded, in general, the smallest shifts in orientation and position from preregistration to postregistration. Nonetheless, the surface-based registration algorithm was able to significantly shift the initially aligned US point clouds to produce a good fit on the CT surface.

To further test the robustness of the ICP algorithm, an examination of the sensitivity of the registration results to initial position was performed. The initial position of the L1, 7.5-MHz fiducial set was shifted in all three directions (x, y, and z) by distances ranging from 1.25 to 10 mm, both positive and negative on a particular axis. For these data sets, a positive shift in x meant displacement to the right; in y, a translation towards the

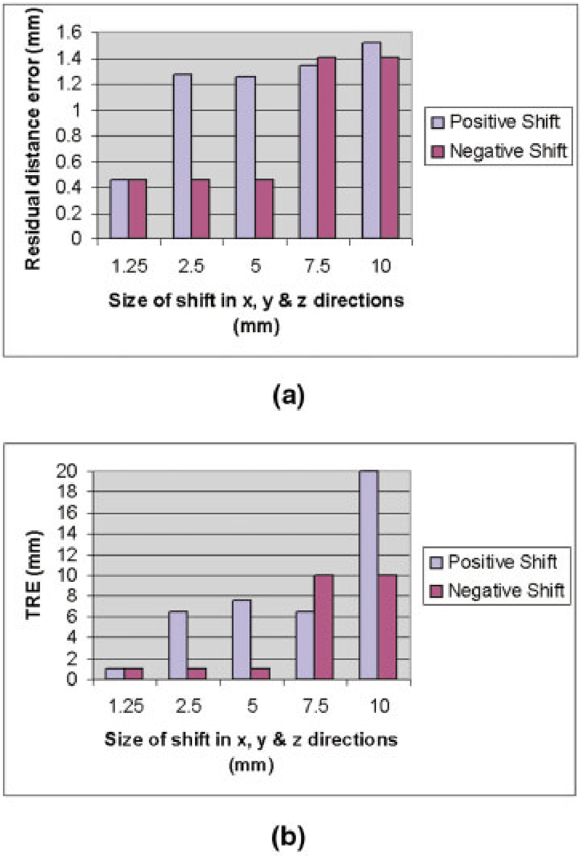

Fig. 8. (a) Residual distance error vs. size of translation of fiducial point set. (b) TRE vs. size of translation of fiducial point set.

vertebral body; and in z, a displacement up the spinal column. Next, the shifted set was placed in the ICP algorithm and allowed to find a solution for alignment with the 2-mm CT surface. The results of this test are presented in Figure 8. The residual fitting errors are plotted in Figure 8a, and the TREs are graphed in Figure 8b. Recall that the original residual error for this registration was 0.46 mm, while the original TRE was 0.98 mm.

The two bar graphs in Figure 8 show that the vertebral point set can be shifted prior to registration by up to 5 mm in the x, y, and z directions—yielding a total displacement of almost 9 mm—and still produce registration results almost identical to those obtained with the original fiducial set. The registration results do not correlate for each positive- and negative-shift pair in Figure 8. One reason for this phenomenon is that the original US fiducial set was only loosely aligned from the start with the CT surface. Consequently, a positive shift of 2.5 mm in all three directions pulled the fiducial point cloud out of a good general alignment, whereas the -5-mm translation in x, y, and z did not.

In addition, this sensitivity study investigated the effect of rotation about the three coordinate axes on registration accuracy. Again, the original fiducial set from L1 at 7.5 MHz was rotated about all three axes over the range 1.25 to 25°, both positively and negatively. The results shown in Figure 9 reveal that nearly equivalent registrations are produced with as much as a 15° rotation about the x-, y-, and z-axes.

An occasional mismatch of the results for the positive- and negative-rotational pairs can be observed in Figure 9. The mismatches in both Figures 8 and 9 occurred where the initial transformation undergone by one set in the pair exceeded the limit of the maximum allowable transformation in the three directions. The transformation of the other set in the pair remained under or closer to the limit for the three reverse directions. In other words, these limits on the transformations were not identical for positive and negative translations or rotations.

The better registration results in aligning the 7.5-MHz data to the 2-mm and 3-mm CT sets can be partially explained by the resolution capacities of the two transducers. The 7.5-MHz images in this study have a spatial resolution of approximately 0.6

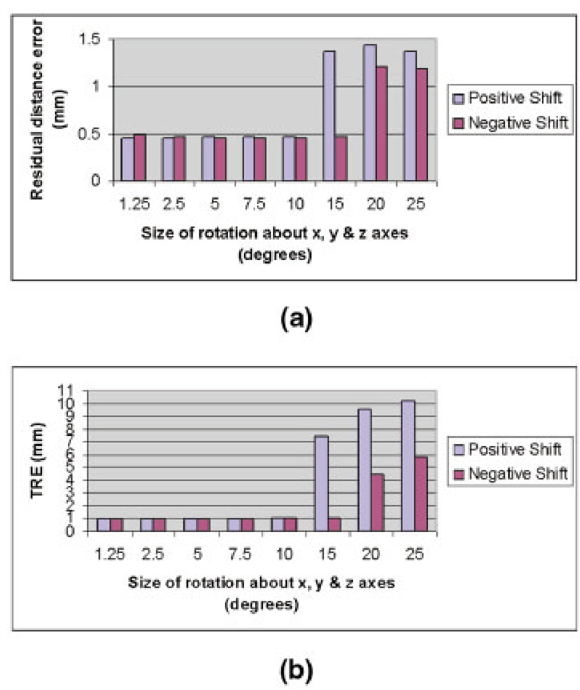

Fig. 9. (a) Residual distance error vs. size of rotation of fiducial point set. (b) TRE vs. size of rotation of fiducial point set.

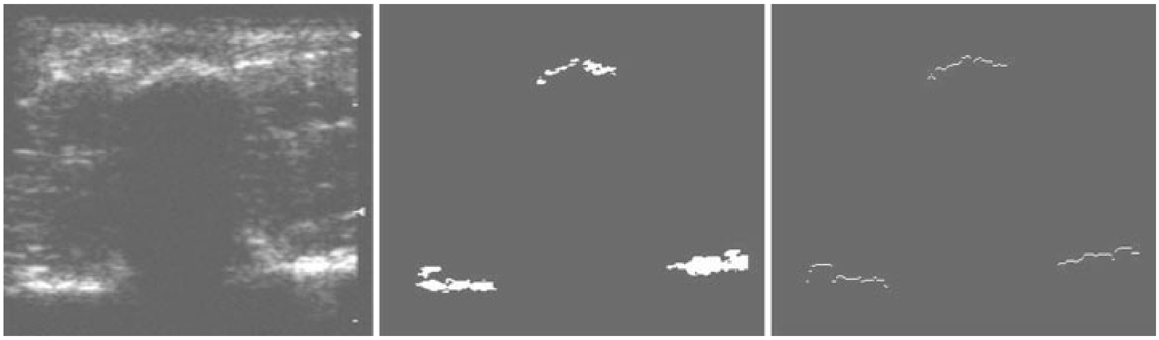

Fig. 10. Left: human lumbar vertebra. Middle: segmented regions of interest. Right: extracted surfaces of the spinous process and laminae.

mm. On the other hand, the 4.5-MHz transducer produces an image with a resolution of just over 1 mm. When the US beam was calibrated, the pixels of the 7.5-MHz beam were better localized because of the higher resolution capacity of the 7.5-MHz transducer. With the higher resolution CT sets, our surface-based registration results indicated that the extracted data from the 7.5-MHz scans produced better TREs than the points extracted from the 4.5-MHz images. We have not yet achieved TREs on the order of the US image resolution, but with projected adjustments to our image acquisition system, we anticipate a reduction in the registration errors for future studies.

A possible explanation for the increase in TRE as CT resolution diminished is the reduced accuracy in localizing the imaging markers. The imaging markers are cylindrical with a diameter of 5 mm and height of 7 mm. In the 2-mm CT set, an imaging marker can be seen in at least three slices. In the 5-mm CT set, however, an imaging marker potentially can fall in just one slice. Thus, an accurate localization of the markers is very dependent on image resolution, and the suspected inaccuracies in marker localization using the lower resolution images could affect the reliability of our gold-standard transformation.

Three-dimensional point localization using the optical tracking system is limited to an accuracy of roughly 0.3 mm. Moreover, the reliability of a TRE measure is affected by marker geometry.[21] With these effects in mind, the fiducial markers were placed in a configuration that minimized potential errors due to a faulty geometrical layout. Interestingly, some of the TREs generated from our surface-based registrations with the 2-mm CT set were near to the best error reported in studies using point-based registrations. At this point, a TRE of 0.7 mm, obtained using optical tracking and a fiducial marker system, is the ultimate measure for the gold standard in a point-based registration. Therefore, we can conclude that TREs in our best-case phantom registration trials have approached this value.

An important consideration at this point would be the clinical validity of our registration results. According to the *Report of the Image-Guided Spine Procedures Workshop*, the desired accuracy for preoperative planning of a trajectory for entry into the spinal area is about 1 mm.[22] Moreover, the navigation into the spinal region is expected to be accurate to within 2 mm.[23] Our results have begun to demonstrate this kind of expected accuracy, although we must account for the ideal nature of phantom trials. In this application, the percutaneous localization of vertebral structures by aligning extracted US points to CT surfaces would be sufficiently accurate for clinical use if we can mimic our best experimental results with clinical data.

Also of interest from the above-mentioned *Report* is the recommended time for intraoperative image segmentation. The research team advocates no more than 5 min of processing time for intraoperative image segmentation.[22] The segmentation routines used in this work also meet this recommendation, transforming raw US images to 3D US surface points in roughly 2 min for a set of 90 US scans. This surface extraction procedure has also been tested in a clinical environment, and, with slight modification, continues to extract the proper ROIs. The modifications are necessary to handle the additional image features such as skin, muscle, fat, and nerves that appear in an *in vivo* image. Figure 10 shows a view of an *in vivo* human lumbar vertebral image (left) along with the segmented

ROIs (center) and the extracted surface points (right).

The choice of transducer frequency was influenced by the interest in prospective clinical applications. The 4.5-MHz transducer offers better signal penetration but lower image resolution than the 7.5-MHz transducer. Because an acoustic signal more rapidly attenuates at higher frequencies, the selection of an optimal transducer is dependent on the depth of the target tissue. For the majority of soft-tissue abdominal scans, the best balance between resolution and penetration is achieved with transducers in the range of 3.5–4.5 MHz.[24] However, the use of US for scanning bone is atypical, and for our application the acoustic signal will only need to travel as deep as the laminar surface. Therefore, we anticipate that the better resolution afforded by the 7.5-MHz transducer will allow for better registrations in clinical settings.

The good registration results achieved in this preliminary study are encouraging for our future work. Using a tracked, free-hand US transducer, extracted surface points from vertebral US images were localized in 3D. This cloud of US vertebral surface points was successfully aligned to CT triangulated surfaces using an independent implementation of the Besl-McKay ICP algorithm. Accurate registrations, particularly using a 7.5-MHz transducer and 2-mm CT scans, were possible with only part of the vertebral surface. This work is distinctive in that free-hand, tracked US images and CT images, acquired from an entire, nonisolated phantom spine, were aligned by using segmented vertebral surfaces. This procedure for registering US to CT has the added advantage of having a trusted, independent measure of accuracy. Although the imaging marker system for accuracy estimation is not intended for clinical use in our application, it offers validation of these phantom studies.

The residual errors reported in this work are consistent with, and even an improvement over, those found in other IGS studies. In addition, the residual errors support the fact that surface alignment from US to CT is more accurate at higher CT resolutions, in particular at 2- and 3-mm slice thicknesses. The CT resolution will, therefore, be an important consideration for *in vivo* experimental design. In those registration trials with the highest CT resolution, TRE reached clinically acceptable numbers. Granted, these trials were undertaken on a phantom, but, given the ability of our US segmentation algorithm to robustly handle human data, the conversion to 3D volume sets will readily proceed from here. Clinical studies of this nature are planned in which we will examine the effect of the additional noise and anatomical features in clinical US images on localization accuracy.

Merging our technological developments with minimally invasive spinal procedures may improve the efficiency and cost of spinal therapies while reducing the invasiveness of these procedures. With over a quarter of a million lumbosacral spinal surgeries being performed annually,[25] new technology is in demand from spinal surgeons. Consequently, research efforts are rapidly expanding in this area. Development of image registration techniques for IGS of the spine may improve the delivery of treatment to patients and may make this therapy affordable for a greater number of patients.

ACKNOWLEDGMENT

This research was funded through NIH Grant GM 52798. Special thanks are extended to Jim Stefansic for use of his image-grabbing software; Andy Bass for assistance in calibrating the US rigid body; Tuhin Sinha for use of his version of the US image processing algorithm; Steve Hartmann and Mark Bray for help with the geometrical transformations; Steve Gebhart, Xiaochun Wang, Ryan Beasley, and Dave Cash for assistance with data collection; and Valerie Futral for her collaboration in designing the prototypical rigid body.

REFERENCES

1. Kimia B, Bullitt E, Arata L, Gregerson G, Liu A, Liu Y, Loew M, Navab N, Rampersaud YR, Wang J, Wells W, Yoo T, Zeng J, Zheng Q. Registration and segmentation. In: Cleary K, editor: Technical Requirements for Image-Guided Spine Procedures Workshop Report. Washington, DC: Georgetown University Medical Center, 1999. p 25–30.
2. Maintz JBA, Viergever MA. A survey of medical image registration. Med Image Anal 1998;2:1–37.
3. Herring JL, Dawant BM, Maurer CR, Muratore DM, Galloway RL, Fitzpatrick JM. Surface-based registration of CT images to physical space for image-guided surgery of the spine: a sensitivity study. IEEE Trans Med Imaging 1998;17(5):743–752.
4. Glossop ND, Hu RW, Randle JA. Computer-aided pedicle screw placement using frameless stereotaxis. Spine 1996;21(17):2026–2034.
5. Steinmann JC, Herkowitz HN, El-Kommos H, Wesolowski DP. Spinal pedicle fixation: confirmation of an image-based technique for screw placement. Spine 1993;18:1856–1861.
6. Carl AL, Khanuja HS, Sachs BL, et al. In vitro simulation: Early results of stereotaxy for pedicle screw placement. Spine 1997;22:1160–1164.
7. Kalfas IH, Kormos DW, Murphy MA, McKenzie RL,

Barnett GH, Bell GR, Steiner CP, Trimble MB, Weisenberger JP. Application of frameless stereotaxy to pedicle screw fixation of the spine. J Neurosurg 1995;83:641–647.

8. Nolte L-P, Zamorano LJ, Jiang Z, Wang Q, Langlotz F, Berlemann U. Image-guided insertion of transpedicular screws. Spine 1995;20(4):497–500.
9. Bolger C, Wigfield C, Melkent T, Smith K. Frameless stereotaxy and anterior cervical surgery. Comp Aid Surg 1999;4(6):322–327.
10. Lavallée S, Troccaz J, Sautot P, Mazier B, Cinquin P, Merloz P, Chirossel J-P. Computer-assisted spinal surgery using anatomy-based registration. In: Taylor RH, Lavallée S, Burdea GC, Mösges R, editors: Computer Integrated Surgery: Technology and Clinical Applications. Cambridge, MA: MIT Press, 1996. p 425–449.
11. Tonetti J, Carrat L, Lavallée S, Pittet L, Merloz P, Chirossel JP. Percutaneous iliosacral screw placement using image guided techniques. Clin Orthop 1998; 354:103–110.
12. Pagoulatos N, Edwards WS, Haynor DR, Kim Y. Interactive 3-D registration of ultrasound and magnetic resonance images based on a magnetic position sensor. IEEE Trans Info Tech Biomed 1999;3(4):278–288.
13. Muratore DM, Galloway RL. Beam calibration without a phantom for creating a three-dimensional freehand ultrasound system. Ultrasound Med Biol 2001; 27(11):1557–1566.
14. Wang MY, Maurer CR, Fitzpatrick JM, Maciunas RJ. An automatic technique for finding and localizing externally attached markers in CT and MR volume images of the head. IEEE Trans Biomed Eng 1996; 43:627–637.
15. West JB, Fitzpatrick JM, Wang MY, Dawant BM et al. Comparison and evaluation of retrospective intermodality brain image registration techniques. J Comp Assist Tomogr 1997;21:554–566.
16. Guéziec A, Hummel R. Exploiting triangulated surface extraction using tetrahedral decomposition. IEEE Trans Visual Comp Graphics 1995;1:328–342.
17. Herring JL, Dawant BM. Automatic identification of a particular vertebra in the spinal column using surface-based registration. In: Taylor C, Colchester A, editors: Proceedings of Second International Conference on Medical Image Computing and Computer-Assisted Intervention (MICCAI'99), Cambridge, UK, September 1999: Lecture Notes in Computer Science 1679. Berlin: Springer, 1999. p 613–620.
18. Lorensen WE, Cline HE. Marching Cubes: A high resolution 3-D surface construction algorithm. Comp Graphics 1987;21(4):163–169.
19. Besl PJ, McKay ND. A method for registration of 3-D shapes. IEEE Trans Pattern Anal Machine Intell 1992; 14:239–256.
20. Maurer CR, Fitzpatrick JM, Wang MY, Galloway RL, Maciunas RJ, Allen GS. Registration of head volume images using implantable fiducial markers. IEEE Trans Med Imaging 1997;16:447–462.
21. West JB, Fitzpatrick JM, Toms S, Maurer CR Jr., Maciunas RJ. Fiducial point placement and the accuracy of point-based, rigid-body registration. Neurosurgery 2001;48:810–817.
22. Tendick F, Polly D, Blezek D, Burgess J, Carignan C, Higgins G, Lathan C, Reinig K. Operative planning and surgical simulators. In: Cleary K, editor: Technical Requirements for Image-Guided Spine Procedures Workshop Report. Washington, DC: Georgetown University Medical Center, 1999. p 25–30.
23. Duerk JL, Grönemeyer D, Bascle B, Clarke L, Deli M, Devey G, Herman W, Hum B, Kim Y, Rosenbaum A, Watson V, Zinreich SJ. Intraprocedural imaging and endoscopy. In: Cleary K, editor: Technical Requirements for Image-Guided Spine Procedures Workshop Report. Washington, DC: Georgetown University Medical Center, 1999. p 33–46.
24. Krautkramer-Branson, Inc. Axial Resolution and Lateral Resolution. Aero-Tech Reports, 1978.
25. Hood RS. Far lateral lumbar disc herniations. Neurosurg Clinics N Am 1993;4(1):117–124.